

Facial Signature Authentication Using Thermal Images

V. Gangadhara Achari¹ S. Raghavendra Swami², S. Ravi Kumar³

¹PG Scholar, Electronics and Communication Engineering,
PVKK Institute of Technology AP, India

²Asst Professor, Electronics and Communication Engineering,
PVKK Institute of Technology, AP, India

³Asst Professor, Electronics and Communication Engineering,
PVKK Institute of Technology, AP, India

Abstract: A new thermal imaging framework with unique feature extraction and similarity measurements for face recognition is presented. The research premise is to design specialized algorithms that would extract vasculature information, create a thermal facial signature, and identify the individual. The proposed algorithm is fully integrated and consolidates the critical steps of feature extraction through the use of morphological operators, registration using the Linear Image Registration Tool, and matching through unique similarity measures designed for this task. The novel approach at developing a thermal signature template using four images take at various instants of time ensured that unforeseen changes in the vasculature over time did not affect the biometric matching process as the authentication process relied only on consistent thermal feature. To achieve more reliable verification or identification we should use something that really characterizes the given person. Biometrics offer automated methods of identity verification or identification on the principle of measurable physiological or behavioural characteristics such as a fingerprint or a voice sample. The characteristics are measurable, unique and these characteristics should biometrics not be duplicable.res.

Index Terms: Biometric, face recognition, image registration, image segmentation, thermal imaging.

1. INTRODUCTION

Biometrics is a technology used for measuring and analyzing a person's unique characteristics. There are two types of biometrics: behavioral and physical. Behavioural biometric is generally used for verification. While physical biometric is used for either identification or verification. Biometrics is the science of using digital technology to identify individuals based on the individual's unique physical and biological qualities. Simply, biometrics is the technique of verifying a person's identity from a physical characteristic (i.e., fingerprint, hand print, face, scent, thermal image, or iris pattern), or personal trait (voice pattern, handwriting, or acoustic signature). The use of thermal mid-wave infrared (MWIR) portion of the electromagnetic (EM) spectrum solves the problem of light variability. Also, any foreign object on a human face such as a fake nose could be detected, as foreign objects have a different temperature range than that of human skin. Due to these benefits, a lot of effort has been aimed at developing human face recognition systems in the MWIR spectrum. However, since cameras in the MWIR portion of EM spectrum are available at a much higher cost than their visible band counterparts, much of the research done in human face recognition in the MWIR spectrum is still in its infancy.

In this study, we extend this research by presenting an integrated approach that consolidates unique algorithms at extracting thermal imaging features, producing templates that rely on the most consistent features, and matching these features through newly developed similarity measures for authentication. Given the complex nature of human vasculature, this approach to face recognition using MWIR imaging is checked against another existing database to prove the reliability of the algorithms designed for feature extraction, template generation, and authentication through similarity measures.

2. MATERIALS AND METHODS

The work presented in this study consists of three major modules: 1) collection of MWIR images, 2) feature extraction, and 3) feature matching. In each of these modules, different instructive steps and safeguards starting from camera calibration to facial thermal signature extraction are taken to ensure

that authentication is made through features that are consistent through several image acquisition times and are therefore more likely to be part of the vasculature of the individual.

A. Collection of MWIR Images

Data collection was accomplished using the Merlin MWIR camera system which operates in the MWIR of the EM spectrum. For this study, we collected thermal infrared images from 13 different subjects. The Merlin MWIR camera was placed on a tripod at a distance of 1 m from the subject who is asked to sit on a fixed chair to facilitate the picture-taking process. The recording of the thermal infrared images was done in a room with an average room temperature of 23 °C. Each subject was asked to sit straight in front of the thermal infrared camera and asked to look straight into the lens and a snapshot of their frontal view was taken. This process was repeated at least three more times in different days and times of the day to take into consideration subtle variations that may occur over time. The time gap for acquisition of the images among and within subjects varied from a period of a week for some subjects up to three months for others.

B. Feature Extraction

Once a thermal camera is calibrated, one of the most challenging tasks of any biometric system is the feature extraction process, which in the final analysis should mimic in the best way possible the human facial vasculature. The premise is that facial skin temperature is closely related to the underlying blood vessels; thus by obtaining a thermal map of the human face, we can also extract the pattern of the blood vessels just below the skin. Thermal feature extraction from facial images was attained by performing morphological operations such as opening and top-hat segmentation to yield thermal signatures for each subject. Four thermal images taken over a period of six months were used to generate a thermal signature template for each subject to contain only the most prevalent and consistent features. In this study, consistent features are defined as those features which are present in three or more thermal signatures obtained from an individual's images taken at different times. A detailed explanation of extracting these consistent features is provided in Section II-B2e.

An important contribution at this stage of the process is in the way unique templates are generated for each individual, which through anisotropic diffusion and unique registration processes create facial signatures that encompass the most consistent features recorded over time. This is an essential step that ensures that facial authentication is carried out with success. Fig.1 displays the flowchart of the entire procedure showing the steps required for the feature extraction process to generate features templates which will then be matched against any facial signature as input to the system.

1) Thermal Infrared Image Registration: Image registration is a challenging task in the field of image processing. Various techniques are available for image registration for medical images and for images in biometric applications [12]–[14]. The intrasubject image registration of the acquired thermal infrared images was performed using the FMRIB Software Library (FSL). The image registration process was achieved using the Analysis Group at the Oxford Center for functional magnetic resonance imaging (MRI) of the Brain's (FMRIB's) Linear Image Registration Tool (FLIRT), assuming the rigid body model option for 2-D image registration. FLIRT has been shown to be significantly faster and accurate in image registration as compared to other techniques such as simulated annealing of the genetic algorithms for MRI applications [15], [16]. However, the specific use of FLIRT for registering thermal facial images as presented in this study has not been addressed in the literature to the best of our knowledge.

Four images from each subject were used in the registration process, whereby one was chosen as the reference image and the rest were registered to the reference image. The thermal image of the subject is taken at different times, and therefore, slight lateral and vertical shifts in the position of the subject relative to the camera's position are experienced. The purpose of the registration process is to account for any lateral and/or vertical movement from the subject that could have taken place during data collection. This simplifies the overlay of the signatures and templates, and makes similarity measurements more meaningful.

The FLIRT registration of images greatly depends on the parameters chosen for the registration task. The various parameters that need to be addressed are 1) cost function, 2) degrees of freedom (DOF), and 3) interpolation. The choice of the cost function depends on the nature of the image to be registered in terms of size and gray scale, relative to other images. Also, since both the input and the

reference images in this case are of the same modality, a within-modality cost function has to be employed to obtain better results. It was found that for thermal images under consideration, the “mutual information” cost function gave us the best registration results. Mutual information formulation used for the registration of the thermal images was first suggested in [17] and [18]. The mutual information is the combination of three different entropies. These include the separate entropies of the two images to be registered as well as their joint entropy.

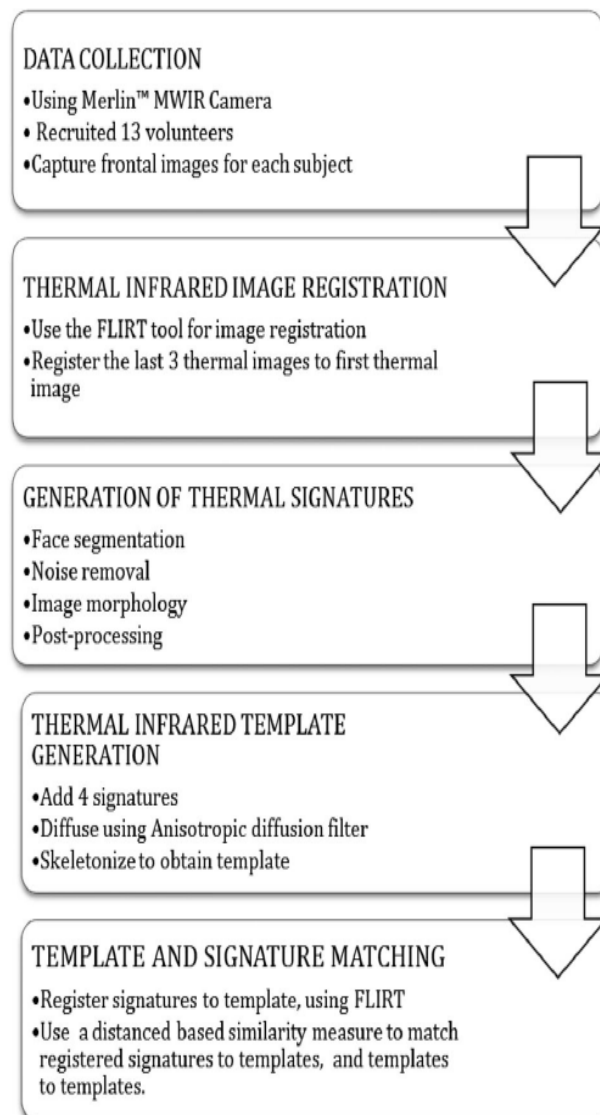


Fig.1. Flow diagram of the entire thermal-signature-based biometric recognition approach

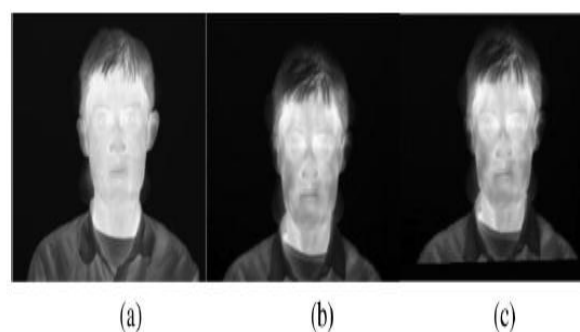


Fig.2. Results of thermal image registration procedure. (a) Reference image. (b) Image to be registered. (c) Registered image after using the developed registration technique.

Four DOF are chosen for the study: one each for the two dimensions of the image, one for rotation, and one for the scaling. The FLIRT algorithm is employed thus using 4 DOF to achieve a complete

registration between the two images. The interpolation step of the process is only used for the final transformation, not in the registration calculations. Various types of interpolations can be used, but since the images are fairly aligned with only slight shifts in position, a nearest neighbor interpolation was found to be sufficient. Fig. 2 shows the results of the registration process for one of the subjects. Notice how the registered image is shifted up in order to correctly register the image to the reference image.

2) Thermal Signature Extraction: After registering the thermal images for each subject, we proceeded to extract the thermal signature in each image. The thermal signature extraction process has four main sections: face segmentation, noise removal, image morphology, and post processing.

a) Face segmentation: In this step, the face of the subject was segmented from the rest of the image. The segmentation process was achieved by implementing the technique of localizing region-based active contours in which typical region-based active contour energies are localized in order to handle images with non-homogeneous foregrounds and backgrounds [19], [20]. The face region segmented here does not take into consideration the neck of the person. This is achieved by localizing the contouring algorithm to a neighborhood around the point of interest with a localization radius of 5 pixels. Since some subjects tended to wear clothing that obstructed the neck region area, we opted not to include that region for uniformity in the segmentation process as well as in performing the similarity measurements to involve only the face.

Let $\Psi = \{x/\Phi(x) = 0\}$ be a closed contour of interest. The interior of the closed contour Ψ is expressed in terms of the smoothed approximation of the signed distance function given Fig. 3. Results of the segmentation process showing the original thermal image and the face segmented image.

as

$$\Phi(x) = \begin{cases} 1, & \Phi(x) < -\varepsilon \\ 0, & \Phi(x) > \varepsilon \\ \frac{1}{2} \left\{ 1 + \frac{\Phi}{\varepsilon} + \frac{1}{\pi} \sin \frac{\pi\Phi(x)}{\varepsilon} \right\}, & \text{otherwise} \end{cases} \quad (1)$$

where $\Phi(x)$ is a smoothed initial contour and $[-\varepsilon, \varepsilon]$ represents the boundary of the Heaviside function in (1). In reference to (1), the exterior of the closed contour is given as $\{1 - H\Phi(x)\}$.

In order to model the energies of the interior and exterior of the contour for face segmentation purposes, the well-known energy is used. The energy defines a dual-front active contour, which is widely used for segmentation purposes in cases where the solution may fall in a local minima and yield poor results.

The algorithm operates by first dilating the user-selected initial contour to create a potential localized region R for finding the optimal segmentation. Thus

$$R = \Phi \oplus S \quad (2)$$

where S is a spherical structuring element of the localization radius (i.e., 5 pixels) and \oplus is the dilation operator. The algorithm proceeds by evolving the inner and outer boundaries of R to reach minima where the inner and outer boundary contours intersect after applying a single iteration of the algorithm called the dual-front active contour region growing technique. The newly formed intersection acts as a new initialization and the process is repeated until the energy function is minimum. Fig. 3 shows the original thermal image and the resultant image after the segmentation procedure. It can be seen that the algorithm successfully segments out the face removing the neck and the hair region from the face.

b) Noise removal: After the face was segmented from the rest of the thermal infrared image, we proceeded to remove unwanted noise in order to enhance the image for further processing. A standard Perona Malik anisotropic diffusion filter is first applied to the entire thermal image.

The significance of the anisotropic diffusion filter in this particular application is to reduce spurious and speckle noise effects seen in the images and to enhance the edge information for extracting the thermal signature. For the diffusion filter, a 2-D network structure of eight neighboring nodes (north, south, east, and west, northeast, northwest, southeast, and southwest) is considered for diffusion conduction. The conduction coefficient function used for the filter applied on the thermal images aims to privilege edges over wider regions in order to enhance regions of high thermal activity associated with the thermal signature. Thus, the conduction coefficient function used for the application is given by

$$C(x, y, t) = \frac{1}{1 + \left(\frac{\|\nabla I\|}{K} \right)^2} \quad (3)$$

where ∇I is calculated for the eight directions and K is the gradient modulus threshold that controls the conduction and avoids the blurring of facial features.

c) Image morphology: Image morphology is a way of analyzing images based on shapes. In this study, we assume that the blood vessels are a tubule-like structure running along the length of the face. The operators used in this experiment are opening and top-hat segmentation, which are detailed next. The effect of an opening operation is to preserve foreground regions that have a similar shape to the structuring element or that can completely contain the structuring element, while eliminating all other regions of foreground pixels. The opening of an image can be described mathematically as follows:

$$I_{\text{open}} = (I \ominus S) \oplus S \quad (4)$$

where I and I_{open} are the face segmented image and the output opened image, respectively; \ominus and \oplus are the morphological erosion and dilation operators.

The top-hat segmentation has two versions; for our purpose, we use the version known as white top-hat segmentation as this process enhances the bright objects in the image; this operation is defined as the difference between the input image and its opening. The selection of the top-hat segmentation is based on the fact that we desire to segment the regions associated with those of higher intensity, which demark the facial thermal signature. The task in this step is to enhance the maxima in the image. The top-hat segmented image I_{top} is thus given by

$$I_{\text{top}} = I - I_{\text{open}}. \quad (5)$$

d) Post processing: After obtaining the maxima in the image, the skeletonization process is used to reduce the foreground regions into a skeletal remnant that largely preserves the extent and connectivity of the original region. This is a hemitropic skeletonization process whereby a skeleton is generated by image morphing using a series of structural thinning elements from the alphabet.

Morphological thinning is defined as a hit-or-miss transformation which is essentially a binary template matching where a series of templates L_1 through L_8 are searched throughout the image. A positive search is annotated as 1 and a miss as 0. This annotation is the result of the following mathematical expression:

$$I_{\text{skel}} = I_{\text{top}} | (I_{\text{top}} \hat{x} L_i) \quad (6)$$

where \hat{x} is the hit-or-miss operator and L_i is the set of structuring elements L_1 through L_8 . The first two structuring elements used



Fig.4. Result of the signature extraction procedure. (a) Original thermal image. (b) Thermal signature

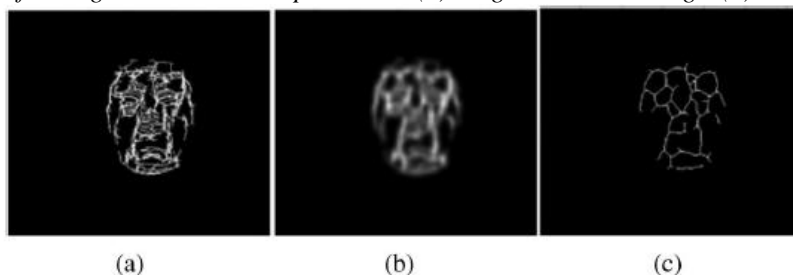


Fig.5. Generation of thermal signature template. (a) Resultant image of addition of four thermal signatures. (b) Results of applying anisotropic diffusion on summed image. (c) Thermal signature template of the subject.

for the skeletonization process are shown as follows:

$$L_1 = \begin{bmatrix} 1 & 1 & 1 \\ 0 & 1 & 0 \\ 0 & 0 & 0 \end{bmatrix}, \quad L_2 = \begin{bmatrix} 0 & 1 & 0 \\ 0 & 1 & 1 \\ 0 & 0 & 0 \end{bmatrix}. \tag{7}$$

The rest of the six structuring elements can be obtained by rotating both the masks L_1 and L_2 by 90° , 180° , and 270° . Fig. 4 shows the resultant image after the post processing approach. The image shown in Fig. 4(b) is referred to here as the thermal signature of that particular subject.

e) Generation of thermal signature template: Thermal signatures in an individual vary slightly from day to day due to various reasons like exercise, environmental temperature, weight, health of the subject, temperature of the imaging room, and many more. Taking into consideration the various factors that may affect the thermal signature; the proposed approach relies on establishing a thermal signature template that preserves those characteristics in a person’s thermal signature that are consistent over time.

The generation of a thermal signature template consists of taking the extracted thermal signatures for each subject and adding them together. The resulting image is a composite of four thermal signature extractions, each one slightly different from the other. The goal is to keep the features that are present in all the images as the dominant features that otherwise define best the individual signature. We then apply an anisotropic diffusion filter to the result of the added thermal signatures in order to fuse the predominant features.

These different steps together with the final template that is sought are illustrated in Fig. 5. For all future testing purposes, a database of the templates is created against which any newly acquired thermal signature image is tested. Fig. 6 shows some illustrative examples on how the thermal signature templates are overlaid on the thermal image of the corresponding subject.



Fig.6. Illustrative thermal templates overlaid on the thermal image of the corresponding subject

C. Distance-Based Similarity Measure for Thermal Infrared Signatures and Template Matching

Similarity measures are widely used in applications like image databases, in which a query image is a partial model of the user's desires and the user looks for images similar to the query image. In our study, we make use of similarity measures because we are attempting to find a thermal infrared template similar to the query thermal infrared signature. Given a thermal infrared signature A (non reference image), and a thermal infrared template B (reference image), the similarity measure between A and B , denoted by $S(A \rightarrow B)$, is defined as follows:

$$S(A \rightarrow B) = \sum_{i=1}^h \frac{1}{h(D_i + 1)} \quad (8)$$

where $1/h$ is the weight associated in matching a single feature (or thermal pixel). Parameter h denotes the minimum number of feature points found in either A or B , i.e., $h = \min(N_A, N_B)$, where N_A and N_B are the number of features in A and B , respectively. Parameter h is the maximum number of features that we could obviously match. The parameter D_i is the minimum Euclidean or Manhattan distance between the i th feature point in B and its closest feature point in A . In finding D_i , the distance of all features in A to those in B are computed, thus creating a vector containing h Euclidean distances for every feature point. The two features that correspond to the minimum distance in the vector are then matched; this process continues until all h features are considered. Also, when two or more features in A match the same feature in B , it means that two or more features in A are equidistant to B . In such a case, we decided to take the first feature in A and match it to B .

It is to be noted that the similarity measure defined in the study obeys the property of symmetry as long as the image with the minimum number of features (h) is referred to as the reference window or reference image.

In addition to computing similarities with the skeletonized templates of the subject, we calculated the similarities between the diffused versions of the signatures and templates. The motive behind generating a diffused template and comparing to it was to see if minor errors resulting due to misalignment of the images have an impact on the similarities.

3. CONCLUSION

This paper has presented a novel approach for biometric facial recognition based on extracting consistent features from multiple thermal infrared images. The approach used FLIRT for thermal image registration and localized-contouring algorithms to segment the subject's face. A morphological image processing technique was developed to extract features from the thermal images, thus creating thermal signatures; these signatures were used to create templates which were then matched using similarity measures. The matching between templates and signatures was done twice using a similarity measure based on 1) the Euclidean distance and 2) the Manhattan distance. Using the Euclidean-based similarity measure, we obtain 88.46% accuracy for skeletonized signatures and templates; for anisotropically diffused signatures and templates, we obtain 90.39% accuracy. Using the Manhattan-based similarity measure, we obtain 90.39% accuracy for skeletonized signatures and templates.

REFERENCES

- [1] M. Adjouadi, T. Barot, R. Bhatt, M. Goryawala, M.R. Guillen, S. Gulec, A. McGoron, and R. Suthar, "A new 3D liver segmentation method with parallel computing for selective internal radiation therapy," *IEEE Trans. Inf. Technol. Biomed.*, vol. 16, no. 1, pp. 62–69, Jan. 2012.
- [2] V. K. Asari and S. Gundimada, "Facial recognition using multisensory images based on localized kernel eigen spaces," *IEEE Trans. Image Process.*, vol. 18, no. 6, pp. 1314–1325, Jun. 2010.
- [3] M. Bazakos, P. Buddharaju, I. T. Pavlidis, and P. Tsiamyrtzis, "Physiology based face recognition in the thermal infrared spectrum," *IEEE Trans. Pattern Anal.*, vol. 29, no. 4, pp. 613–626, Apr. 2009.
- [4] J. Bronzino, Ed. Boca Raton, FL: CRC Press, 2006. M. Khader and A. Ben Hamza, "Nonrigid image registration using an entropic similarity," *IEEE Trans. Inf. Technol. Biomed.*, vol. 15, no. 5, pp. 681–690, Sep. 2011.

- [5] B. Brunsten, C. Hildebolt, L. J. Larson-Prior, T. S. Nolan, M. Pringle, F. W. Prior and S. N.Vaishnavi, , “Facial recognition from volume rendered magnetic resonance imaging data,” *IEEE Trans. Inf. Technol.Biomed.*, vol. 13, no. 1, pp. 5–9, Jan. 2009.
- [6] T.Chau and B.R.Nhan, “Classifying affective states using thermal infrared imaging of the human face,” *IEEE Trans. Biomed. Eng.*, vol. 57, no. 4, pp. 979–987, Apr. 2010.
- [7] X. Q. Dai , K. X. Deng, J.Tian , M.Xu, X. Zhang and J.A.Zheng, “Salient feature region: A new method for retinal image registration,” *IEEE Trans. Inf. Technol. Biomed.*, vol. 15, no. 2, pp. 221–232, Mar. 2011.